International Journal of Automotive Technology, Vol. 8, No. 2, pp. 233–241 (2007)

1229-9138/2007/033-13

MODELING AND PARAMETER IDENTIFICATION FOR A PASSIVE HYDRAULIC MOUNT

Y. X. ZHANG[1)*], J. W. ZHANG[1)], W.-B. SHANGGUAN[2)] and Q. SH. FENG[3)]

[1)]School of Mechanical Engineering, Shanghai Jiao Tong University, Shanghai 200240, China
[2)]School of Vehicle Engineering, South China University of Technology, Guang Zhou 510641, China
[3)]Purchasing department, Shanghai General Motors Corporation Limited, Shanghai 201206, China

(Received 4 September 2006; Revised 22 January 2007)

ABSTRACT–A lumped parameter model is proposed for the analysis of dynamic behaviour of a Passive Hydraulic Engine Mount (PHEM), incorporating inertia track and throttle, which is characterized by effective and efficient vibration isolation behaviour in the range of both low and high frequencies. Most of the model parameters, including volume compliance of the throttle chamber, effective piston area, fluid inertia and resistance of inertia track and throttle are identified by an experimental approach. Numerical predictions are obtained through a finite element method for responses of dynamic stiffness of the rubber spring. The experiments are made for the purpose of PHEM validation. Comparison of numerical results with experimental observations has shown that the present PHEM achieves good performance for vibration isolation.

KEY WORDS : Passive hydraulic engine mount, Lumped parameter model, Parameter identification, Dynamic response

1. INTRODUCTION

Undesirable vibrations for engine mounts generally result from two possible excitation sources. The first is engine oscillation, which typically contains frequencies in the range of 25~200 Hz with amplitudes generally less than 0.3 mm. The second originates from road inputs and engine torque during harsh accelerations, with frequencies under 30 Hz and amplitudes over 0.3 mm (Singh and Kim, 1992). Accordingly, the engine mount serves two main functions: power train support and bi-directional vibrations isolation. Rubber mount was the primary method of vibration isolation since 1930s; however, it could not meet more stringent requirements, especially for the non-linear excitation situation. Through past research, the theory of the engine hydraulic mount can be classified into the following two directions: Passive Hydraulic Engine Mount (PHEM) and Active Hydraulic Engine Mount (AHEM). PHEM is widely used in the automotive industry in view of good dynamic response and low cost. Problems of PHEM, including modeling, performance estimation and system identification, have drawn more and more researchers' attention.

Different PHEM configurations result in diverse dynamic responses and in general, the more complex the PHEM structure, the better the PHEM dynamic behaviour becomes. Using linear mathematic models and counting for an open or closed decoupler, Flower analyzes dynamic behaviour of the hydraulic mount (Flower, 1985). Mechanical models for a single-pumper are proposed; dynamic stiffness equations are derived by Nader and apply a bond-graph analysis method (Nader, 2005). The approach uses quasi- and non-linear mathematical models for hydraulic mount analysis; an inertia track and a decoupler is presented by Singh and Kim (Singh and Kim, 1992; Kim and Singh, 1995). Following Singh's modeling method, a number of experiments were designed for parameter recognition by Geisberger, Khajepour and Golnaraghi (Geisberger *et al.*, 2002). Although the above research introduced the whole vehicle for the first time and broadened the predicted system bandwidth, by the numerical predictions mentioned above, such a type of configuration of the hydraulic mounts has undesirable dynamic behaviour in the high frequencies range. The overall behaviour and fluid-structure interaction for the Finite Element Method (FEM) of the hydraulic engine mounts containing a floating decoupler, was investigated by Wen-Bin Shangguan and Zhenhua Lu (Shangguan and Lu, 2004a) using integration of mathematical estimation and experimental verification.

The hydraulic mounts mentioned above showed great improvements on the dynamic performance of rubber mount in the low frequency range, thus meeting the increasing customer demand for a quieter and smoother

*Corresponding author. e-mail: yunxia_8@hotmail.com

riding performance. However, an unexpected stiffness rigidification in the high frequency range was found. Theoretic and experimental research proves that hydraulic mounts with an inertia track and/ or decoupler could not meet the high frequency excitation. In order to improve the performance of a high frequency engine mount, a novel hydraulic engine mount incorporating inertia track and throttle is introduced in this paper. A lumped parameter model of the engine mount, capable of capturing both the low- and high-frequency behaviour of PHEM, is developed. The parameters are identified by experimental approach and the Finite Element Analysis (FEA) method. In addition, the model is also validated by experimental data.

2. LUMPED PARAMETER MODEL

A cross-section of the PHEM is depicted in Figure 1(a) in detail. The mount is comprised of three chambers with different volumes, termed the throttle and upper and lower chambers, respectively. The PHEM dynamic model with lumped parameters is shown in Figure 1(b). The

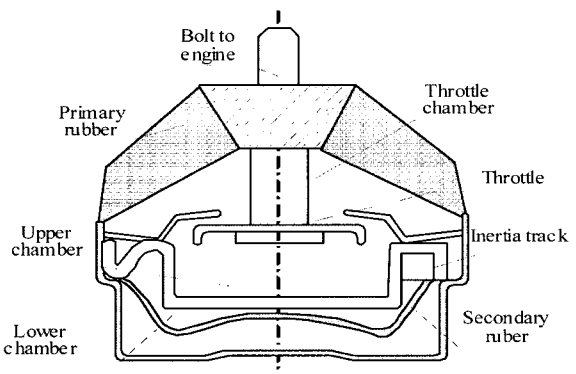

(a) Cross section and configuration

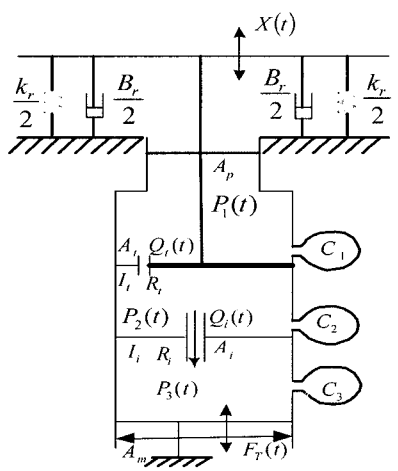

(b) Lumped parameter dynamic model

Figure 1. The PHEM with inertia track and throttle.

definition of parameters for the dynamic model is given as follows: C_1, C_2 and C_3 are compliances of the three chambers respectively; K_r and B_r represent dynamic stiffness and the damping coefficient of the rubber spring; A_p is an equivalent piston area of the rubber spring, A_t is total area of orifices around the throttle plate and A_m is the area of the mount at the throttle; I_i is the fluid inertia in the inertia track lumped parameters; R_i represents the resistance coefficient of the fluid in the inertia track; I_t and R_t represent inertia and resistance of the throttle with lumped parameters, respectively; $Q_i(t)$ and $Q_t(t)$ represent flows passing through the inertia track and the throttle, respectively; $P_1(t)$, $P_2(t)$ and $P_3(t)$ represent pressures in the throttle, the upper and the lower chambers respectively. $X(t)$ is input displacement excitation and $F_T(t)$ is transfer force to the mount base.

2.1. Linear Model

Mathematic modeling is essential in order to understand the dynamic response of the mount system. Complex and precise non-linear models are usually derived from linear ones. This section describes the linear model for the typical operation mode. The dynamic equations for the lumped model can be derived according to continuity and momentum equations. The continuity equations for each of the chambers can be expressed as follows:

$$C_1\dot{P}_1=Q_t-(A_m-A_t-A_p)\dot{X} \tag{1}$$

$$C_2\dot{P}_2=(A_m-A_t)\dot{X}-Q_t-Q_i \tag{2}$$

$$C_3\dot{P}_3=Q_i \tag{3}$$

The momentum equations for each of the fluid system can be presented in the following forms as:

$$P_2-P_1=I_t\dot{Q}_t+R_t(Q_t+A_t\dot{X}) \tag{4}$$

$$P_2-P_3=I_i\dot{Q}_i+R_iQ_i \tag{5}$$

And the transmitted force equation is:

$$F_T=k_rX+b_r\dot{X}+(A_m-A_t)(P_2-P_3)+ A_mP_1+A_iR_iQ_i-(A_m-A_p)P_1 \tag{6}$$

2.2. Non-linear Model

Enhanced parameters for the linear model are usually employed while developing the non-linear PHEM model. These parameters include non-linearity the inertia track resistance and throttle resistance, R_{i1} and R_{t1}. It follows from reference (Geisberger *et al.*, 2005) that non-linearity of the rubber spring in stiffness and damping characteristics, effective piston area and volumetric compliance are considered in the model. The momentum equation for the throttle becomes:

$$P_1-P_2=I_t\dot{Q}_t+(R_t+R_{t1}|Q|_t)Q_t+F_t/(A_m-A_t) \tag{7}$$

When the free throttle reaches the top end, all liquid in the top chamber flowing through the throttle is blocked and the force of the throttle is expressed as follows (Christopherson and Jazar, 2006):

$$F_t=E\left(\frac{x}{\Delta}\right)^{\gamma}\dot{x}_t \tag{8}$$

where E is a positive constant, γ is a positive odd constant, x_t is the displacement of the throttle, Δ is the moving interval of the throttle, and F_t is the force on throttle.

The non-linear momentum equation for the inertia track becomes:

$$P_2-P_3=I_i\dot{Q}_i+(R_i+R_{i1}|Q_i|)Q_i \tag{9}$$

3. PARAMETRIC IDENTIFICATIONS OF THE HYDRAULIC MOUNT

Numerical model's parameters are identified by experimental approaches, whereby components of the hydraulic mount are isolated to enable parameter identification. The parameters needed in the following simulations include: C_1, A_p, I_i, R_i, I_t, R_t and K_r.

3.1. Identification of Equivalent Piston Area and Volumetric Compliance

The experimental apparatus for identifying the effective area and volumetric compliance is shown in Figure 2 (Shangguan, 2003). The actuator position is connected to actuator of the MTS 831 elastomer test system. During experimental preparation, ethylene glycol, specified as the customer requirements, is filled into the liquid chamber under the vessel, ensuring no air bubble in chambers. The displacement excitation at the actuator position pushed fluid into the sample chambers. Measurements of mount displacement, actuator position and vessel pressures, etc. are tabulated and then processed to determine the above parameters. Other experiment layouts involved in this paper are similar to Figure 2.

The volume compliance C_1 in Figure 2(a) can be expressed as:

$$C_1\dot{P}_s=Q_a \tag{10}$$

where, Q_a is introduced to represent the flow entering the compliant region. P_s is the feedback pressure of the sensor.

The flow is calculated as the derivative (with time) of the volume excitation:

$$Q_a=\dot{V}_{actual} \tag{11}$$

where V_{actual} is the flow volume of the actual position:

$$C_1\dot{P}_s=\dot{V}_{actual} \tag{12}$$

To transform the equation into the frequency domain,

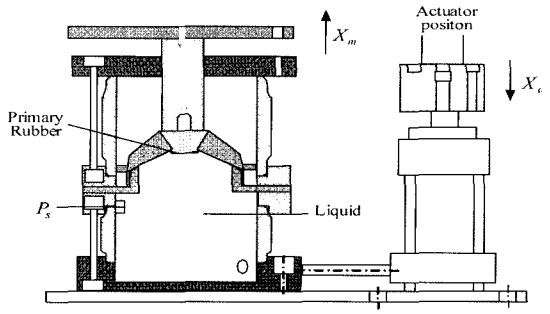

(a) Test configuration

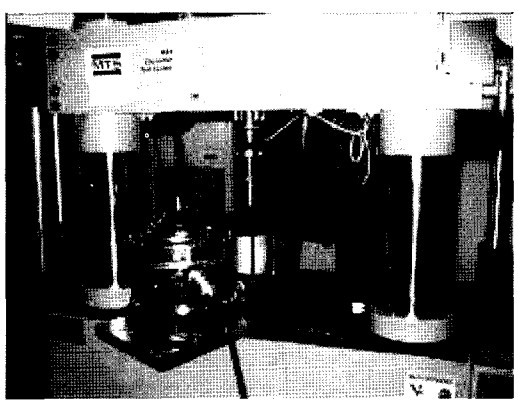

(b) Photo for Test bench

Figure 2. Test instruments for parameter identification: the effective area and volumetric compliance parameters.

the final frequency domain equation becomes:

$$\frac{\tilde{P}_s}{\tilde{V}_{actual}}=\frac{1}{C_1} \tag{13}$$

where, $\tilde{P}_s$ and $\tilde{V}_{actual}$ are the phase and amplitude of complex pressure and volume respectively.

The volume can be expressed by the product of the action area of the piston, A_{piston} and the actual displacement X_a, in which X_a can be measured in the experiment:

$$\tilde{V}_{actual}=\tilde{X}_a A_{piston} \tag{14}$$

Then Equation (13) becomes:

$$\frac{\tilde{P}_s}{\tilde{X}_a A_{psiton}}=\frac{1}{C_1} \tag{15}$$

Thereby the parameter C_1 is identified using the measured frequency domain data, including the pressure sense P_s and the actual displacement X_a. By substituting the experimental data, the compliance curve vs. frequency is obtained and shown in Figure 3a. The fit value for C_1 is 3.0×10^{-11} m^5/N.

Effective piston area A_p can be calculated as follows:

$$A_p X_m=A_{piston} X_a \tag{16}$$

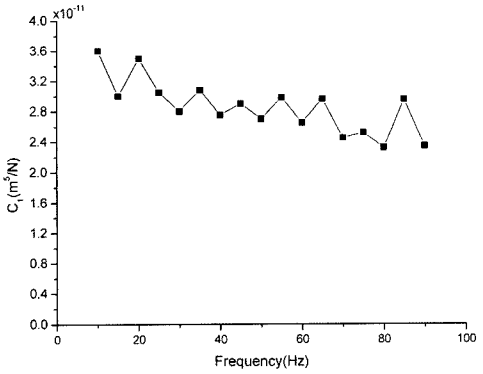

(a) Volume compliance

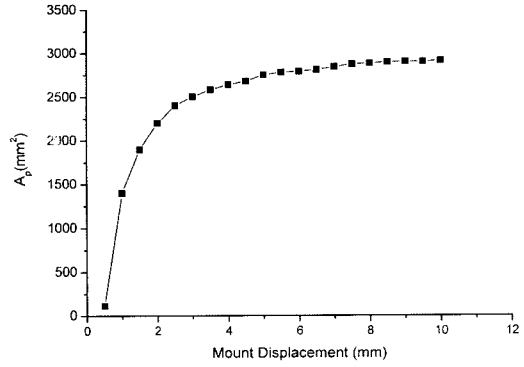

(b) Effective piston area

Figure 3. Curves of volume compliance and effective piston area.

To simulate actual work conditions of the engine mount, a 900N force is applied as a preload to the experimental sample, thus the mount displacement X_m and the action position displacement X_a are measured. The curve of A_p vs. mount displacement is plotted in Figure 3b. In range of 0~3 mm, A_p increase with displacement and the curve finally reaches a stable trend of 2500 mm^2 in the range of 5~10 mm.

3.2. Identification of Inertia Track Parameters

The momentum nonlinear equations for inertia track is:

$$P_s=I_i\dot{Q}_i+(R_{i1}+R_{i2}|Q_i|)Q_i \tag{17}$$

Where, R_{i2} is the resistance parameter on squared flow across the inertia track.

The isolated response follows a linearized form of Equation (17):

$$P_s=I_i\ddot{V}_{actual}+R_i\dot{V}_{actual} \tag{18}$$

Transformation form in the frequency domain of Equation (18) is:

$$\frac{\Delta\tilde{P}_s}{\tilde{V}_{actual}}=-I_i\omega^2+R_i\omega j \tag{19}$$

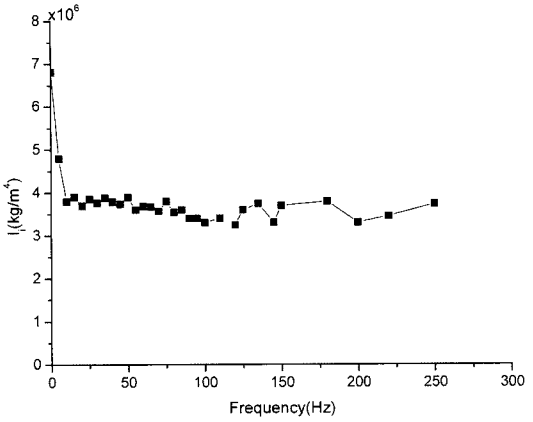

(a) Fluid inertia

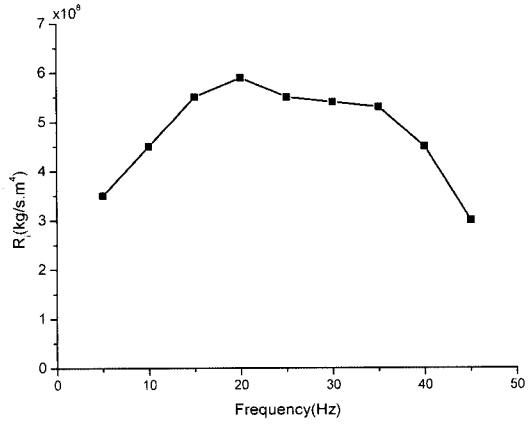

(b) Resistance coefficient (low frequency)

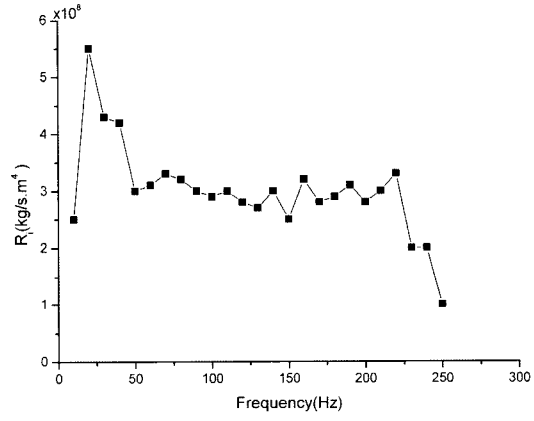

(c) Resistance coefficient (high frequency)

Figure 4. Curves of fluid inertia and resistance coefficient for inertia track.

The linear parameters of the inertia track can be identified by equation (19) and curves for the above two parameters are illustrated in Figure 4. The different flow resistance of the inertia track is noticed in different excitation conditions. According to the curves, I_i is obtained as 3.8×10^6 kg/m^4. R_i is 5.5×10^8 kg/s.m^4 for the

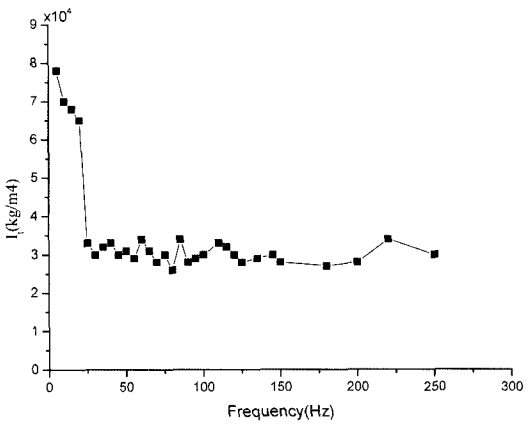

(a) Throttle inertia

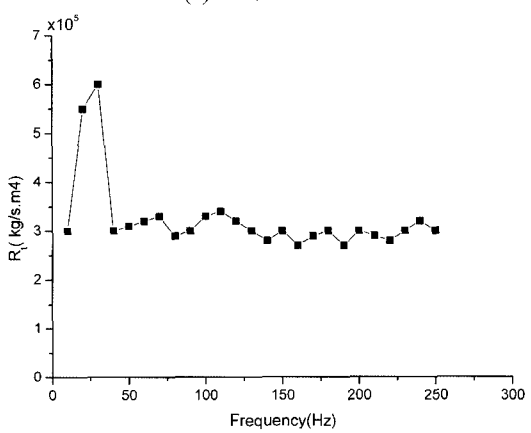

(b) Throttle resistance

Figure 5. Curves of inertia and resistance of the throttle.

mode of low frequency with large amplitude, or 3×10^8 kg/s.m^4 for the mode of high frequency with small amplitude, respectively.

3.3. Identification of Throttle Parameters

The momentum nonlinear equations for throttle is:

$$P_s=I_t\dot{Q}_{actual}+(R_{t1}+R_{t2}|Q_{actual}|)Q_{actual} \tag{20}$$

A simplified Equation (20) with the experimentally measured data:

$$\Delta P_s=I_t\ddot{V}_{actual}+R_t\dot{V}_{actual} \tag{21}$$

Transfer Equation (21) into frequency domain:

$$\frac{\Delta\tilde{P}_s}{\tilde{V}_{actual}}=-I_t\omega_{dr}^2+R_t\omega_{dr}j \tag{22}$$

The linear parameters of throttle parameter I_t and R_t can be identified by equation (22). In the same way, the calculated I_t and R_t are plotted in Figure 5. The values for the two parameters adopted in the following simulation are 3×10^4 kg/m^4 and 3×10^5 kg/s.m^4 respectively.

3.4. Identification of Dynamic Stiffness of the Rubber Spring

As an important component of the PHEM, material and geometry of the primary rubber influence not only the static property of PHEM, but also its dynamic performance. An analysis of the rubber spring significantly reveals the dynamic behaviour. The properties of rubber are difficult to predict, due to the nonlinearity and anisotropy, except for the sensitivity to mechanical and temperature property. The parameters, however, were estimated by experiments and mathematic methods in most cases. Considering its irregular shape, a FEA is more suitable to estimate static stiffness and dynamic stiffness K_r as predicted from equation (Geisberger, 2000):

$$K_r=fK_s \tag{23}$$

where K_s is the static stiffness of the rubber spring and f is the dimensionless correction factor in the variety of 1.2 to 1.6. The Ogden material model for incompressible materials is used to describe the rubber performance and analyze the rubber spring stiffness. The model assumes a strain energy density per unit original volume in the following form:

$$U=\sum_{n=1}^{3}\frac{\mu_n}{\alpha_n}(\lambda_1^{-\alpha_n}+\lambda_2^{-\alpha_n}+\lambda_3^{-\alpha_n}-3) \tag{24}$$

where, α_n and μ_n are material constants to be determined through experiments, and λ_i ($i=1, 2, 3$) are the deformation values of the stretch tensor in the three principle directions, and $\lambda_1\lambda_2\lambda_3=1$. The uniaxial stress-stretch relation of the rubber spring material is plotted in Figure 6, according to the Ogden model (Shangguan and Lu, 2004a).

A three-dimensional solid structure of the rubber spring is built, and the finite element mesh is shown in Figure 7a. The constraint condition and load bearing are added to the FEM mesh model according to the PHEM working condition. The compared curves of dynamic stiffness are also shown in Figure 7b. The comparative curves above are in good agreement between FEA estimation and test results.

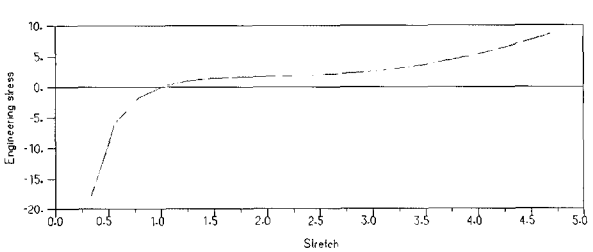

Figure 6. Uniaxial stress-stretch relation of elastic material for the primary rubber.

4. EXPERIMENTAL VALIDATION AND NUMERICAL SIMULATION RESULTS

The dynamic performance of the mount is measured with a MTS 831 elastomer test system. The test sample is clamped on the test bench with a preload of 1000N, similar to a passenger car and in view of accuracy, is applied (as shown in Figure 2). A sinusoidal displacement excitation is applied by a bench actuator for both conditions, as discussed in previous sections. Data for a displacement senor on the actuator and the force sensor from a fixed end are recorded automatically for the further processing and analysis. Detailed descriptions of the experimental method and experimental data processing have obtained the dynamic properties of a mount (Shangguan and Lu, 2004b).

During the identification, the values for inertia track R_i in low frequency with large amplitude are different from that in high frequency with small amplitude. Therefore, the model was simulated using different values for different conditions.

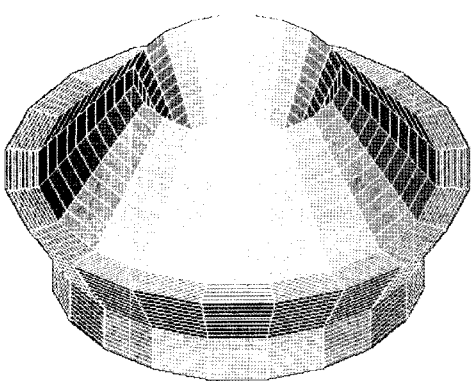

(a) Mesh idealization for FEA

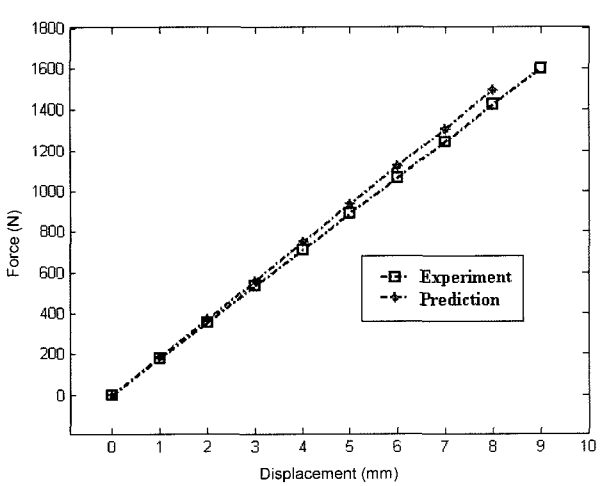

(b) Vertical force-displacement curves

Figure 7. Dynamic stiffness identification for primary rubber spring.

As discussed in previous sections, the typical excitations for the PHEM assembled in the vehicle are classified into two types: low frequency range (1~50 Hz) with large amplitude (1 mm) and high frequency range (0~200Hz) with small amplitude (0.1 mm). Accordingly, the dynamic responses are shown in Figure 8 and Figure 9 as a solid line. To obtain relative differential equations and frequency response characteristics from the non-linear model, the equations are solved in a time domain and then converted to the corresponding frequency domains with MATLAB.

Using the lumped parameter model in Section 2 and identified parameters in Section 3, the simulated results and experimental data for the mount dynamic behaviour are compared over the frequency range of 1~50 Hz and 1~200 Hz. The predicted dynamic stiffness and loss angle spectra of the mount for low frequency with high ampli-

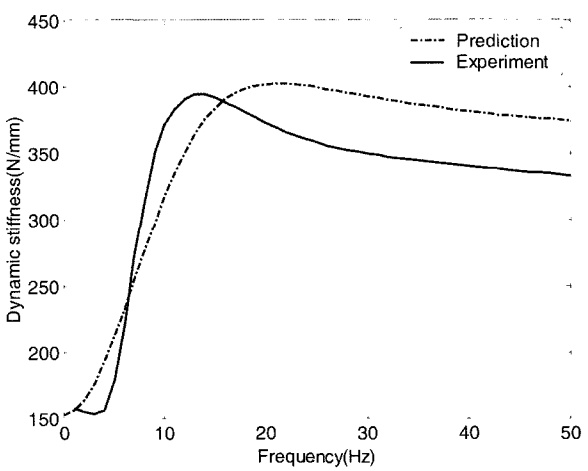

(a) Dynamic stiffness

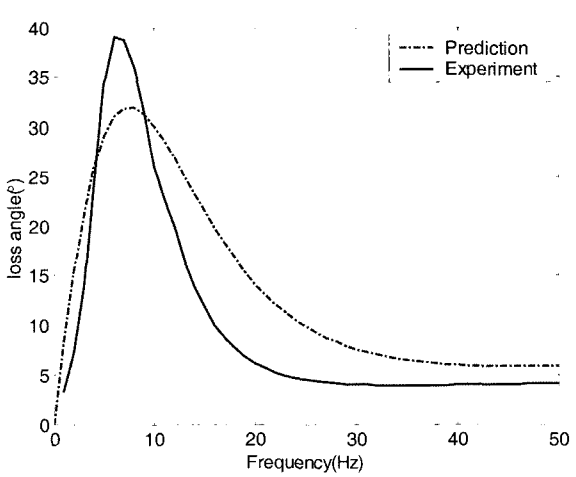

(b) Loss angle

Figure 8. Comparisons of the numerical predictions with experimental results for the dynamic responses of the mount in a low frequency domain with large amplitude.

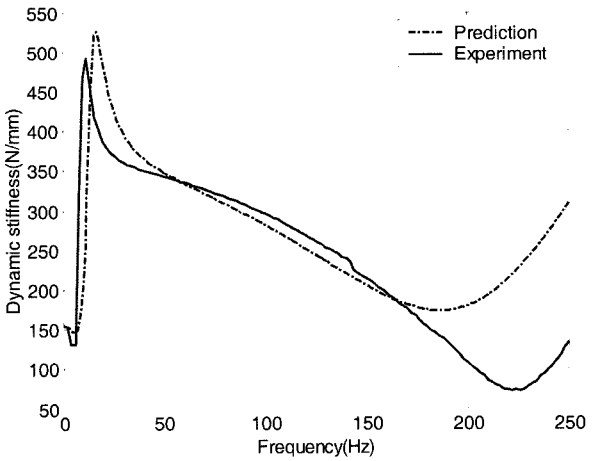

(a) Dynamic stiffness

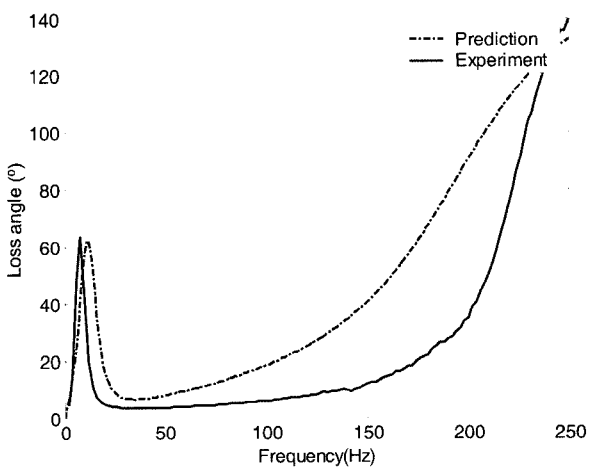

(b) Loss angle

Figure 9. Comparisons of the numerical predictions with experimental results for the dynamic responses of the mount in high a frequency domain with small amplitude.

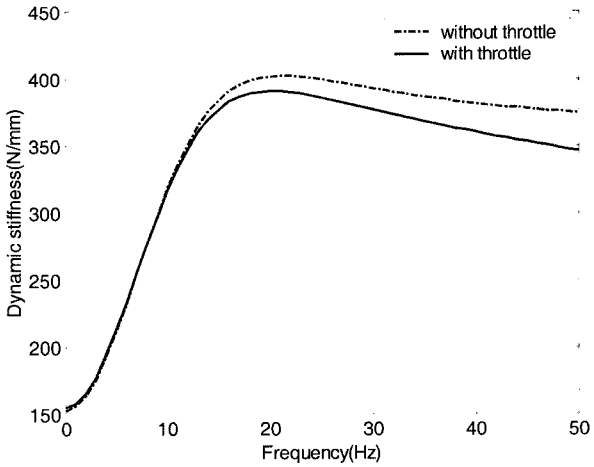

(a) Dynamic stiffness

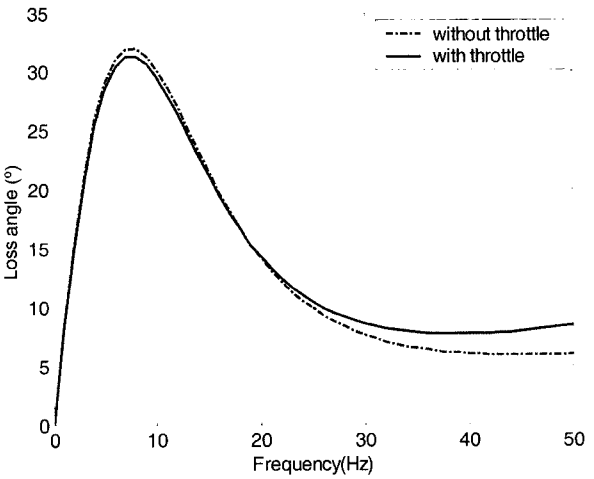

(b) Loss angle

Figure 10. Comparisons of the numerical predictions with throttle and without throttle for the dynamic responses of the mount in a low frequency domain with large amplitude.

tude excitation are shown in Figure 8 by a dashed line. Comparatively, the experimental curves are plotted in solid lines. The dynamic stiffness difference between the predicted and the experimental curves in Figure 8a are not obvious, while Figure 8b tends to indicate fair agreement of loss angle between the two curves. The difference between experiment and simulation curves may have various reasons. The parameters, such as chamber compliance, and a resistance coefficient are fixed values in simulation, while these parameters are changing with excitation frequency and amplitude.

A similar situation between predicated and simulated curves is found in the high frequency with low amplitude excitation mode, as shown in Figure 9. Peak dynamic stiffness appears at 24Hz and then declines with frequency, which shows an obvious advantage versus preceding configurations, in terms of stiffness rigidification in high frequency range. The agreement of the frequency in peak loss angle and the lowest frequency of the dynamic stiffness surging is not significant. The expansion of the stiffness should definitely improve the isolation of high frequency vibration from the internal combustion engine, a highly sought after goal for researchers and vehicle manufacturers.

In order to reveal the function of throttle introduced in the PHEM, comparisons of the numerical predictions with and without throttle for the dynamic responses of the mount are carried out. Furthermore, two typical work conditions, low frequency with large amplitude and high frequency with small amplitude are considered.

The complex stiffness of inertia track is expressed as follows (Zhang *et al.*, 2006):

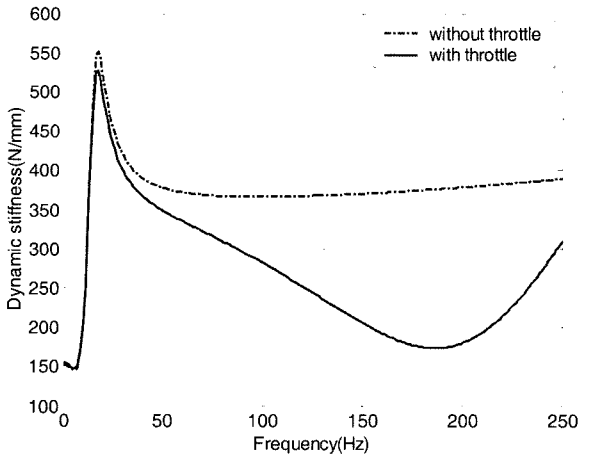

(a) Dynamic stiffness

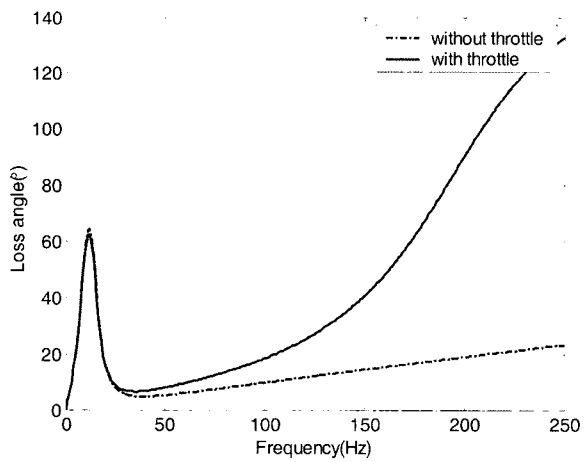

(b) Loss angle

Figure 11. Comparisons of the numerical predictions with throttle and without throttle for the dynamic responses of the mount in a high frequency domain with small amplitude.

$$K=k_r+b_r s+A_p^2 K_1 \frac{I_i s^2 + R_i s}{I_i s^2 + R_i s + K_1} \tag{25}$$

where K_1 is volume stiffness, $K_1=\dfrac{1}{C_1 + C_2}$.

Comparison curves of the numerical predictions are shown in Figure 10 and Figure 11. Figure 10 shows the throttle does not affect the dynamic response in a condition of low frequency with large amplitude. Both dynamic stiffness and loss angle are the same between PHEM without throttle and PHEM with throttle. As indicated in Figure 11, the dynamic stiffness of PHEM with throttle is smaller than the PHEM without throttle in 30~250 Hz of a high frequency domain with small amplitude. The adoption of throttle in the PHEM, as in comparison with a decoupler in the past layout, improves the dynamic stiffness and loss angle in high frequency range, i.e. the frequencies bandwidth of the mount is extended to cover high frequencies.

Therefore, the PHEM with inertia track and throttle reduced vibration, depending on a liquid flow through the inertia track in low frequency with large amplitude. Both inertia track and throttle work together in high frequency with small amplitude; the inertia track R_i became smaller so that the dynamic stiffness and loss angle become large in 0~30 Hz. The dynamic performance depends on throttle in 30~250 Hz.

5. CONCLUSION

The scope of this contribution is to introduce a PHEM configuration in which a throttle is applied relative to previous structures. From the discussion, one may conclude that introduction of throttle provides improvement for dynamic behaviour in a range of high frequency, compared to the past configurations. Moreover, the lumped parameter modeling and identification are carried out, which are integrated into linear and non-linear models of PHEM. In addition, the accuracy of the non-linear model for describing dynamic characteristics has been compared to the experimental results, according to the two typical exciter modes. The works presented here provide valuable research of the PHEM in non-linear aspects.

ACKNOWLEDGEMENTS–The authors gratefully acknowledge the financial support of the Natural Science Foundation of China (Project No. 50575073), the science fund of State Key Laboratory of Automotive Safety and Energy (Project KF2006-06), and the Guangdong Natural Science Foundation (Project No. 04300111). Experiments involved in the paper are carried out in Ningbo Tuopu NVH R&D Center. Helpful discussion and support from the engineers are kindly appreciated.

REFERENCES

Christopherson, J. and Jazar, G. (2006). Dynamic behavior comparison of passive hydraulic engine mounts. Part 1: Mathematical analysis. *J. Sound and Vibration* **290**, 3, 1040–1070.

Flower, W. C. (1985). Understanding hydraulic mounts for improved vehicle noise. *SAE Paper No.* 850975.

Geisberger, A. (2000). *Hydraulic Engine Mount Modeling, Parameter Identification and Experimental Validation.* M. S. Thesis. University of Waterloo.

Geisberger, A., Khajepour, A. and Golnaraghi, F. (2002). Non-linear modeling of PHEMs: Theory and experiment. *J. Sound and Vibration* **249**, 2, 371–397.

Kim, G. and Singh, R. (1995). A study of passive and adaptive hydraulic engine mount systems with emphasis on non-linear characteristics. *J. Sound and Vibration* **179**, 3, 427–453.

Nader, V. (2005). Double-notch single-pumper fluid mounts. *J. Sound and Vibration*, **285**, 697–710.

Shangguan, W. B. (2003). *A Research on Simulation Techniques for Fluid-structure Interaction Dynamic Characteristics of Hydraulically Damped Rubber Mount*. Ph. D. Dissertation. Tsinghua University.

Shangguan, W. B. and Lu, Zh. H. (2004). Modeling of a hydraulic engine mount with fluid-structure interaction finite element analysis. *J. Sound and Vibration,* **275**, 93–221.

Shangguan, W. B. and Lu, Zh. H. (2004). Experimental study and simulation of a hydraulic engine mount with fully coupled fluid structure interaction finite element analysis model. *Computers and Structures* **82**, **22**, 1751–1771.

Singh, R. and Kim, G. (1992). Linear analysis of automotive hydro-mechanical mounts with emphasis on decoupler characteristics. *J. Sound and Vibration,* **158**, 19–243.

Zhang, Y. X., Zhang, J. W. and Shangguan, W. B. (2006). The dynamic response of a novel passive hydraulic engine mount. *J. Shanghai Jiao Tong University* **40**, **6**, 942–946 (in Chinese).